

Insertion Devices

Several insertion devices (IDs) have been developed at NSRRC. The specifications of these insertion devices are listed in Table 1 and their respective spectra shown in Fig. 1.

The goal of a magnetic structure design is to achieve both high field strength and a high quality field. High field strength can be obtained in a hybrid structure with vanadium permendur poles and Nd-Fe-B magnets. However, superconducting ID provides a higher field than the conventional hybrid structure or the electro-magnet. In our application, the hybrid structure was chosen for the W20, U10, U5, and U9 insertion devices. Due to the nonlinear relative permeability of the iron pole, the variations in the first field integral and in the tune shift of the hybrid structure are much larger than those of the pure magnet structure when the phase of the magnet array is changed. Therefore, the pure structure with Nd-Fe-B magnets was the preferred choice for the EPU5.6.

For the hybrid structure, the thickness of the pole tip should be optimized to avoid excessive pole saturation. Hence, the wedged-poles are shaped with a larger cross section at the pole tip

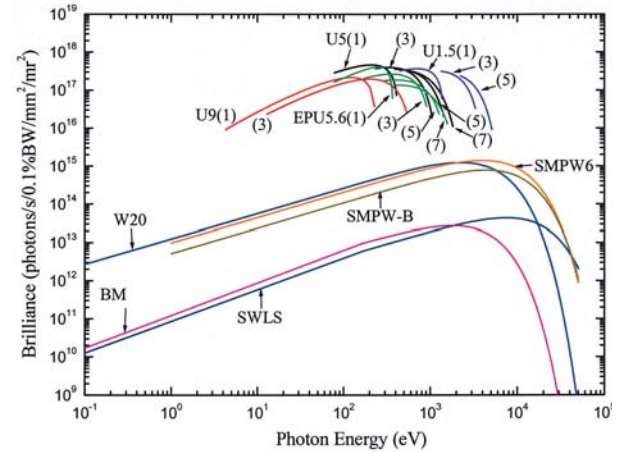


Fig. 1: Spectral brilliance of insertion devices at NSRRC.

(see Fig. 2) of U9. The chamfers shown in Fig. 2 are used to reduce local saturation and demagnetizing fields. Although the vertical recess reduces the field strength, the recess with shims has the effect of minimizing the on-axis field strength variation and maximizing the field-tuning range, such as the case in the U10 design. Magnet overhanging on both vertical and transverse axes

Table 1. Main parameters of NSRRC insertion devices (λ : periodic length; N: periodic number; $\Delta\Theta$: rms spectrum phase error; $\Delta\theta$ and $\Delta\delta$: maximum deviation from the ideal angular and trajectory).

	W20	U10	U5	U9	EPU5.6	SWLS	SMPW6
Type	Hybrid	Hybrid	Hybrid	Hybrid	Pure	Supercon.	Supercon.
λ [cm]	20	10	5	9	5.6	25	6
Gap [mm]	22	22	18	18	18	56	18
N	13	20	76	48	66	1.5	16
B_{\max} [T]	1.8	1.0	0.64	1.25	0.67 (0.45)	6	3.2
Beam duct Aperture (cm ²)	N/A	N/A	N/A	N/A	N/A	2×10	1.2×8
$\Delta\Theta$	N/A	2.5°	3°	3.7°	5.5°	N/A	N/A
$\Delta\theta_x(\Delta\theta_y)$ [μrad]	N/A	15 (6)	6 (11)	20 (10)	10 (15)	N/A	N/A
$\Delta\delta_x(\Delta\delta_y)$ [μm]	N/A	5 (2)	7 (10)	8 (2)	2 (1)	N/A	N/A
Cooling type	N/A	N/A	N/A	N/A	N/A	cryocooler	LHe
Installation	Dec. 1994	Oct. 1995	Mar. 1997	Apr. 1999	Sep. 1999	Apr. 2002	Dec. 2003

shown in Fig. 2 is used to weaken the 3-D leakage flux from the sides of the pole and to reduce the roll-off effect.

A good end pole design should minimize integral dipole strength and reduce trajectory displacement. These criteria were met in the end pole design of EPU5.6 by mounting several small magnet blocks with different thickness on the end poles, as depicted in Fig. 3. The figure also shows that the longitudinal distance between each of the end poles, the pole height, and the pole tilts are all adjustable. At both ends, there are two rows of trim magnet blocks with different sizes for the multipole field shimming. One row is for the normal field and the other one is for the skew field component. The end pole design concept also can be used for other insertion devices. The thin iron (magnet) plates are used for the field shimming of hybrid (pure) magnet structure to correct the trajectory and to reduce the spectrum phase errors. It is better to avoid using shims if magnet swapping can achieve the same results for the linear polarized plane undulators.

Since the cryogenic plant is not available before the middle of 2003, a cryogen-free superconducting wavelength shifter (SWLS) with 6 T

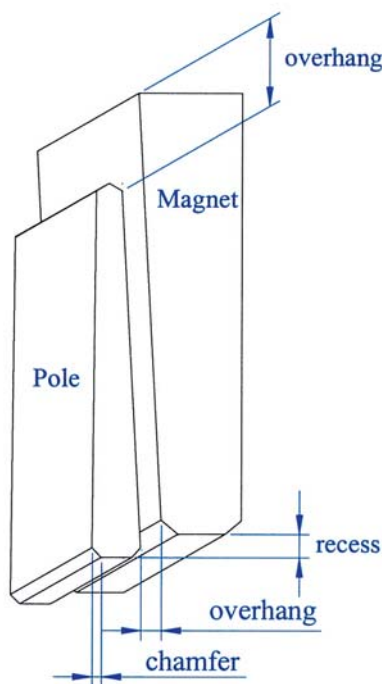


Fig. 2: Schematic drawing of the magnet pole design for hybrid structure insertion devices.

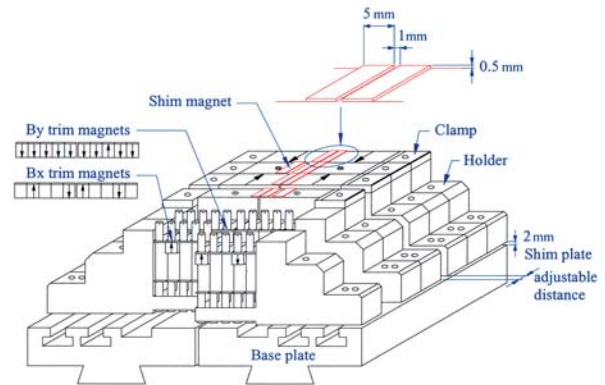


Fig. 3: Schematic drawing of the magnet structure design for the pure undulator, showing the multipole fields trim magnets and the trajectory/spectrum shimming method.

was designed and constructed beginning in 1999 and then installed in the injection straight section in April 2002. The flange-to-flange distance of the SWLS which includes the beam duct taper, the cooling water pipes, and the BPM, is only 835 mm. This magnet is conduction -cooled by a 1.5-Watt GM-type cryo-cooler. The contact surfaces between the conduction parts are carefully jointed together by soft soldering. To reduce vibration from the cryo-cooler, a flexible S-shape OFHC copper connects the 4.2 K and the second stage of cold head. Meanwhile, some damping mechanisms have been considered for the cold head support.

Based on the above design, W20, U10, U5, and U9 have been constructed and optimized to obtain high field strength and a high quality field. For U10, the ratio of photon flux calculated using the measured field to that by the ideal field under zero energy spread at the minimum gap is higher than 80% at the 11th harmonic, indicating a high quality field. The flux density and flux ratio of U10 as a function of the harmonic number (deflection parameter $k=4.6$) are shown in Fig. 4.

The strong back of U9 and U5 is 4.5 m and 4 m long, and the field strength is 1.28 T and 0.64 T at the minimum gap of 18 mm, respectively. The mechanical deformation of the strong back and c-frame is therefore a critical issue. However, the fifth harmonic spectra performance of U5 and U9 are higher than 87% and 95%, respectively. The photon flux ratio of EPU5.6 is calculated using the measured and ideal fields. In the energy range of

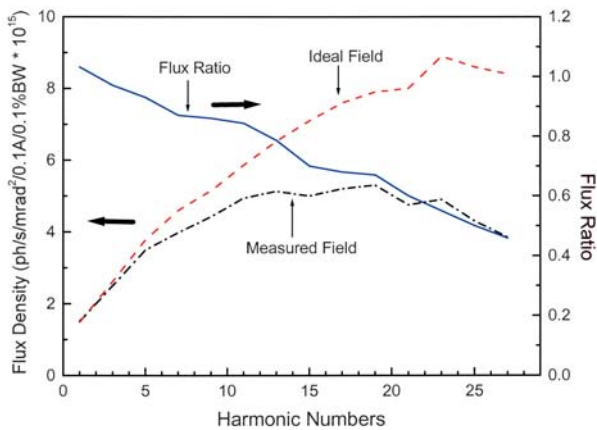


Fig. 4: Photon flux density and flux ratio of U10 as a function of harmonic number.

0.05-1.2 keV, the photon flux ratios of the horizontal (vertical) linear polarization and the right (left) elliptical polarizations were found to be greater than 85% (50%) and 75% (90%), respectively.

Trim correctors located upstream and downstream of the SWLS are used to compensate the multipole components and the first integral field strength. The integral field distribution was measured along the transverse axis after multipole and trajectory shimming. The field distribution can be analyzed to obtain the multipole components and the resulting normal (skew) multipole components, -20 (-20) G-cm, 40 (13) G, -70 (-40) G/cm, -4 (0.5) G/cm² are all close to the specifications. Commissioning of the SWLS took place in May, and the first stored beam with the SWLS operating at 6 T was observed on May 21. Injection with the fully-charged SWLS went smoothly. Compensation of the orbit excursion and tune shift was conducted while increasing the magnetic field and as a result there were no major impacts on the beam dynamics. The measured tune shifts, and path-length compensation, etc., were consistent with the values predicted by model calculation. Vacuum cleaning with synchrotron light was necessary to maintain beam stability and reasonable lifetime. In August, a vacuum leak occurred in the ceramic chamber of the downstream kicker magnet due to insufficient shielding against the powerful synchrotron radiation from the high field SWLS. The shielding was reinforced in October. The beam lifetime during commissioning was limited by the pressure rise, photon

stimulated desorption, mainly from the downstream absorbers. The rate of pressure increase per mA of the electron beam current, and the product of lifetime and beam current. As of March 2003, the accumulation does was 40 Ah and beam lifetime at 200 mA was about 6 hours. At present, the SWLS is routinely operated at 5.3 T without filling liquid He and liquid N₂ and the current slew rate was set at 0.3 A/s when testing the three x-ray beamlines. In the long-term operation, the temperature of magnet and HTS current leads are maintained within 4.3 K and 80.5 K, respectively. In cryogen-free mode, the maximum field of 5.5 T can be obtained at an excitation current of 280 A. The SWLS was capable of operating up to 6.5 T with liquid helium supply.

A superconducting multipole wiggler (SMPW6) will be installed beside the superconducting RF cavity straight-sections. The available space for SMPW6 is 140.56 cm in length. Therefore, 28 effective poles (32 total poles) with periodic length of 6.0 cm were excited up to 3.2 T at the magnet gap of 18 mm. The magnet has been constructed and preliminary results of measured field in vertical dewar are shown in Fig. 5. The measured on-axis field shows that the second field integral is quite good without any correction. A cryogen plant will serve the superconducting insertion devices from 2003. Therefore, the SMPW6 is designed for liquid He operation mode.

There is an increasing demand for intense hard-x-rays at NSRRC in the range from 13 keV to 30 keV from protein crystallography and material science scattering experiments. Although no long straight sections are available for accommodating insertion devices, three achromatic straight sections between BM1 and BM2 can host three shorter superconducting multipole wigglers, SMPW-B, which is similar to the SMPW6. The total length is 0.9 m for the installation of SMPW-B with periodic length of 6 cm and thus 13 effective poles are designed. The main parameters are listed in Table 1. Cold bore beam tube at 4.2 K is used to reduce the magnet gap which will be smaller than 18.5 mm and the magnetic field strength is up to 3.5 T. In addition, there is no extra space to install insertion device unless the W20 is replaced by the superconducting in-

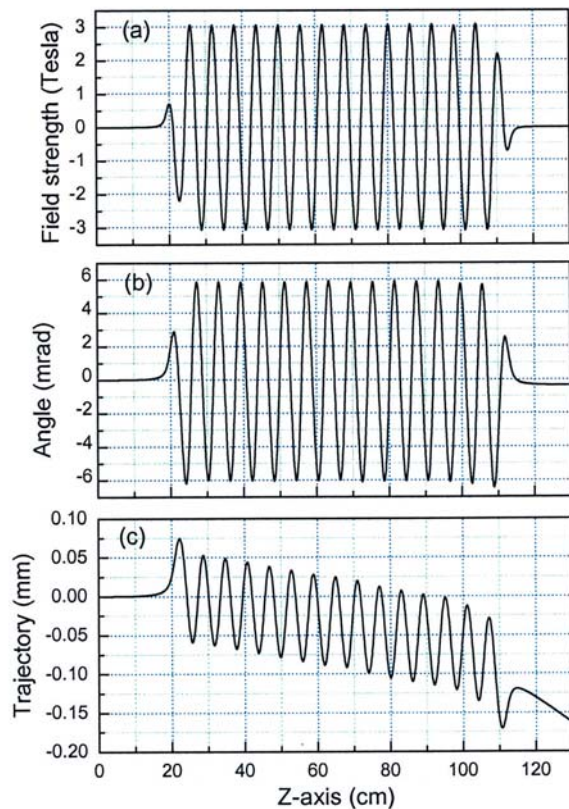


Fig. 5: Preliminary performance of the measured field on vertical dewar: (a) field strength distribution of SMPW6, (b) first field integral and (c) second field integral.

vacuum undulator U1.5. For this reason, the superconducting in-vacuum undulators, racetrack superconducting coil, and stagger type have been studied. The periodic length will be selected at about 15 mm and the field strength is about 1.5 T at magnet gap of 5 mm to match the continuous spectra between 400 eV and 5 keV as shown in Fig. 1.

Author:

C. S. Hwang
National Synchrotron Radiation Research Center,
Hsinchu, Taiwan

Publications:

- C. H. Chang, et al., IEEE Trans. on Magnet **32**, 2629 (1996).
- C. S. Hwang et al., Chinese Journal of Physics **35**, 617 (1997).
- C. S. Hwang et al., Nucl. Instrum. Meth. A

399, 463 (1997).

- C. H. Chang, et al., J. Synchrotron Rad. **5**, 420 (1998).
- C. S. Hwang et al., Rev. Sci. Instrum. **73**, 1436 (2002).
- C. H. Chang, et al., J. Magn. Magn. Mater. **209**, 173 (2000).
- C. H. Chang, et al., IEEE Trans. on Apply Supercond. **10**, 503 (2000).
- C.H. Chang, et al., J. Magn. Magn. Mater. **239**, 363 (2002).
- C. S. Hwang, et al., IEEE Trans. Appl. Supercond. **12**, 686 (2002).
- C. S. Hwang, et al., IEEE Trans. Appl. Supercond. **13**, 1209 (2003).

Contact e-mail:

cshwang@nsrrc.org.tw